

Review

Unraveling the Fate and Transport of DNAPLs in Heterogeneous Aquifer Systems – A Critical Review and Bibliometric Analysis

Abhay Guleria ¹, Pankaj Kumar Gupta ^{2,3,*}, Sumedha Chakma ¹ and Brijesh Kumar Yadav ⁴

¹ Department of Civil Engineering, Indian Institute of Technology Delhi, Delhi 110016, India; abhay_guleria@civil.iitd.ac.in (A.G.)

² Faculty of Environment, University of Waterloo, Waterloo, ON N2L 3G1, Canada

³ Centre for Rural Development and Technology, Indian Institute of Technology Delhi, Delhi 110016, India

⁴ Department of Hydrology, Indian Institute of Technology Roorkee, Roorkee 247667, India

* Correspondence: pk3gupta@uwaterloo.ca

Table S1. List of Top 10 leading countries of DNAPL transport research field.

Country	TCi	Rank based on TCi	AACi	Rank based on AACi	NoA	Rank based on NoA
USA	6856	1	39.63	4	173	1
Canada	2130	2	50.71	1	42	2
United Kingdom	506	3	21.08	8	24	3
Italy	410	4	22.78	7	18	5
Denmark	350	5	31.82	6	11	7
Switzerland	338	6	48.29	2	7	8
China	325	7	13.54	10	24	3
Korea	250	8	35.71	5	7	8
Australia	247	9	41.17	3	6	10
France	235	10	14.69	9	16	6

Table S2 (a). DNAPL contaminated sites in the world.

Sr. No.	Contaminated site	Latitude	Longitude	Country	Maximum Concentration (ppb)
1	Canadian forces base site, Borden, Ontario	44.2899417	-79.8939699	Canada	250000
2	Belfast industrial facility, Northern Ireland	54.597285	-5.93012	United Kingdom	390000
3	Linoleum factory Brunn am Gebirge, Vienna	48.108956	16.2853875	Austria	27
4	Dry-cleaning facility, Rheine, North Rhine-Westphalia	52.2815691	7.4434092	Germany	20000
5	Aircraft maintenance facility, Southern Oregon	42.7976791	-122.4332992	United States of America	500
6	Caldwell Trucking Superfund Site, Northern New Jersey	40.0583238	-74.4056612	United States of America	7000
7	Federal Highway Administration (FHA) Facility, Lakewood, Colorado	39.7091372	-105.1391205	United States of America	700
8	Electromechanical product manufacturing testing facility unit, Fairfield, New Jersey	40.8837406	-74.3059959	United States of America	1200
9	Industrial Site, Coffeyville, Kansas	37.0943823	-95.5819808	United States of America	400
10	Plating Industrial facility, Central New York	43.0510662	-76.1436136	United States of America	1800
11	Former industrial site, Manning, South Carolina	33.6951627	-80.2109134	United States of America	25000
12	Intersil Semiconductor Site, Sunnyvale, California	37.36883	-122.0363496	United States of America	1000
13	U.S. Department of Energy's Plant, Kansas City, Missouri	39.0997265	-94.5785667	United States of America	1377
14	Lowry Air Force Base, Colorado	39.5500507	-105.7820674	United States of America	1400
15	U.S. Coast Guard Support Center site, Elizabeth City, North Carolina	36.2886534	-76.2513495	United States of America	4320
16	Area 5, Dover Air Force Base site, Dover, Delaware	39.1296887	-75.4822875	United States of America	5617
17	Industrial area, Cape Canaveral Air Station, Florida	28.4923776	-80.5768594	United States of America	170000
18	Massachusetts Military Reservation, Falmouth, Massachusetts	41.6636305	-70.5473012	United States of America	300

19	Moffett Federal Airfield, Mountain View, California	37.4090755	-122.0507824	United States of America	2990
20	Savannah River Site TNX Area, Aiken, South Carolina	33.5586735	-81.7234526	United States of America	250
21	SGL Printed Circuits site, Wayne, Passaic County, New Jersey	40.9253725	-74.2765441	United States of America	13000
22	Somersworth Sanitary Landfill Superfund Site, New Hampshire	43.2617503	-70.8653372	United States of America	1900
23	Cannon manufacturing storage unit site, Watervliet Arsenal, Albany, New York	42.7158698	-73.704857	United States of America	4200
24	Portsmouth Gaseous Diffusion Plant disposal facility, Piketon, Ohio	39.0129903	-83.0008687	United States of America	150
25	IBM Dayton site, South Brunswick, New Jersey	40.372607	-74.5101536	United States of America	5500

Table S2 (b). Contaminated sites in India [1,2].

Sr. No.	Name of the Site	Latitude	Longitude	State
1.	Tulsibari, Rangia, District-Kamrup, Assam	26.496658	91.592305	Assam
2.	Bhilai steel plant, Chhattisgarh	21.169611	81.400078	Chhattisgarh
3.	Jhilmil Industrial Area, New Delhi	28.673487	77.31357	Delhi
4.	Gazipur landfill- site, Gazipur, Delhi	28.625153	77.328056	Delhi
5.	Road side and in front of A-5, Lawrence road industrial area-, New Delhi-110032	28.661457	77.295291	Delhi
6.	Mandoli Village, Northeastern Delhi-110093	28.70963	77.31129	Delhi
7.	Open Land adjacent to Ajit Printers B-58 Damodar Park, Dilshad Garden Industrial Area, New Delhi-110052	28.684409	77.31522	Delhi
8.	Open land in front of 77, SSI Industrial Area, New Delhi-110033	28.730974	77.15843	Delhi
9.	Open land which is on back side of Anuradha Petrol Pump and near to C-32, Rajdhani roller flour mill, Lawrence road industrial area, New Delhi-110035	28.683724	77.152642	Delhi
10.	Bhalsawa Landfill, New Delhi-110033	28.740531	77.158673	Delhi
11.	Near Railway Line and Gail No. 4 & 5, New Friends Colony Industrial Area-New Delhi- 110026	28.567462	77.269133	Delhi
12.	Larsen Chem, B/2, Ganeshpura, Opp. Janta Petrol Pump, Modasa Sabar Kantha, Gujarat	23.475619	73.291149	Gujrat
13.	Swastik Organic, Sabar Dairy Road, Piplodi, Gujrat	23.592505	72.972861	Gujrat
14.	Effluent Channel Project Limited (M/s ECPL), Baroda Effluent Canal, Vadodara District	22.342609	73.151402	Gujrat
15.	Hema Chemicals - Unit II (J-71, 72), Nandesari, Vadodara	22.334526	73.162039	Gujrat
16.	Jambusar, District- Bharuch,	22.049444	73.045806	Gujrat
17.	Ankleshwar Industrial Estate, GIDC Industrial Estate, Tal: Ankleshwar, Dist: Bharuch,	21.633139	73.045806	Gujrat
18.	Prem Colony, Kundli Sonapat	28.868137	77.121203	Haryana
19.	Sectors 25 & 29, Dyeing Industry, Panipat, Haryana	29.358608	76.991689	Haryana
20.	Open Space in front of 360E PACE City -2, Sector 37- B Gurgaon-122002	28.436365	76.995535	Haryana
21.	Effluent Drain, Housing Board Phase-III, Baddi, Himachal Pradesh	30.946248	76.812063	Himachal Pradesh

22.	Goripalya near Mysore Road, Bangalore, Karnataka. E- waste recycling in Bangalore, Karnataka	12.964087	77.556605	Karnataka
23.	Mavallipura Dumpsite, Yelahanka, Bangalore	13.122438	77.53775	Karnataka
24.	Kuzhikandom Thodu (Creek), Kerala	10.079547	76.294582	Kerala
25.	Vadavathoor, Kottayam	9.590878	76.559867	Kerala
26.	Edayar, Edayattuchal Kochi, Kerala (in & around the premises of M/s. Binani Zinc Ltd.)	10.08705779	76.30676857	Kerala
27.	Sajjan Chemicals -Plot No ; 54 E dosigoan, Industrial area, Ratlam, Madhya Pradesh	23.357857	75.045467	Madhya Pradesh
28.	Sajjan chemical Pvt Ltd (Plot No -61 B, Dosigaon Industrial Area, Ratlam)	23.360211	75.047161	Madhya Pradesh
29.	M/s Jayant Vitamin, Ratlam	23.330447	75.043353	Madhya Pradesh
30.	Dabli, Mangliya, Indore, MP	22.81521672	75.91170171	Madhya Pradesh
31.	M/s Godavari Bio-Refineries, Ahmed Nagar, District, Maharashtra	19.8233337	74.56901795	Maharashtra
32.	Dumpsite JCL-I (Outside the Premises Of M/S Jayshree Chemicals Ltd Near Rushikulya River)	19.378006	85.051354	Odisha
33.	Dumpsite JCL-III (Outside the Premises Of M/S Jayshree Chemicals Ltd Near Rushikulya River)	19.377793	85.051959	Odisha
34.	Jayashree Chemicals, Ganjam	19.381236	85.052652	Odisha
35.	Site OCL-I, ORICHEM abandoned site (inside the premises of M/s Orichem Ltd and also outside the boundary of wall), Talcher, Orissa	20.925735	85.17287	Odisha
36.	RKL-II (In Beldihi village along the play ground between Govt primary school & St. Georgia school)	22.236011	84.761129	Odisha
37.	Site KCL II, Inside the premises of M/s KCL near Gate, Mayurbhanj, Orissa	21.598039	86.929221	Odisha
38.	Site KCL III, Inside the premises of M/s KCL inside drier room, Mayurbhanj, Orissa	21.597189	86.928847	Odisha
39.	RKL-III (In a low lying area in Kaluga industrial estate near Kalinga Sponge industry, around 500 m away from M/s Konark Chemicals and M/s Siddharth Chemicals)	22.220952	84.769866	Odisha
40.	Site ECFC-I (Backside of the unit.) Mayurbhanj, Orissa	21.603934	86.930121	Odisha

41.	RKL-I (Inside The Premises Of M/S Lotus Chrome Chemicals)	22.234709	84.72228	Odisha
42.	Site INDAL-III (Located outside the unit premises of M/s Indian Aluminum Company Limited), Hirakud, Sambalpur	21.534566	83.912470°	Odisha
43.	Basti Sheikh, Jalandhar	31.320198	75.548062	Punjab
44.	Hambran Road MSW Dump Site, Ludhiana	30.919485	75.753523	Punjab
45.	Buddha Nullah, Ludhiana, Punjab	30.919455	75.90332	Punjab
46.	Mahaluxmi Orgo Chemical Industries, Nabha Road, Bhawanigarh, Sangrur	30.275411	76.074781	Punjab
47.	Tajpur road MSW dump site, Ludhiana	30.928623	75.906736	Punjab
48.	PSIEC Leather Complex, Jalandhar, Punjab	31.332535	75.512237	Punjab
49.	Amanishah nalla, Sanganer Industrial Area, Jaipur	26.817401	75.79004	Rajasthan
50.	Village Bichhadi, Block Girva, Rajasthan	24.589316	73.823643	Rajasthan
51.	M/s HUL, Kodaikanal, Tamil Nadu	10.224714	77.48709	Tamil Nadu
52.	Vanitec Limited (inside the premises of CETP) Vallayambattu, Vadiumbadi, Vellore, Tamil Nadu	12.698153	78.633428	Tamil Nadu
53.	TCCL, Ranipet, Tamil Nadu	12.955092	79.311158	Tamil Nadu
54.	Tondairpet, Chennai, Tamil Nadu	13.12413944	80.28417843	Tamil Nadu
55.	Patancheru, Medak District, Telangana	17.539669	78.245269	Telangana
56.	Khanchandrapuri, Rania Kanpur Dehat	26.403777	80.047415	Uttar Pradesh
57.	Shivnathpura, Rania, (Kanpur Dehat) Ramabai Nagar, Kanpur, Uttar Pradesh	26.413374	80.021637	Uttar Pradesh
58.	Deva Road, Lucknow (Palhauri Village, Deva Road, Chinhat, Lucknow)	26.99668	81.143051	Uttar Pradesh
59.	India Pesticide Limited, Lucknow	26.91415975	81.06959141	Uttar Pradesh
60.	Uttardhauna, Chinhat Block, Lucknow	26.886526	81.055561	Uttar Pradesh
61.	Chakar Village Chinhat, Lucknow	26.926555	81.067481	Uttar Pradesh
62.	Industrial Area Meerut Road, Ghaziabad, Uttar Pradesh	28.685193	77.432472	Uttar Pradesh
63.	Lohia Nagar C Block, Ghaziabad	26.44522	80.322694	Uttar Pradesh
64.	Nauriaya Kheda Kanpur	26.39678	80.43953	Uttar Pradesh
65.	Shakti Nagar, Aligarh	24.229316	83.036038	Uttar Pradesh
66.	Kanoria Chemical Renukoot, Renukoot, Sonebhadra, Uttar Pradesh	29.051893	77.45528	Uttar Pradesh
67.	Barnawa Village, Baghpat, District Meerut	27.1631	78.3733	Uttar Pradesh
68.	Panki Industrial Area, Kanpur	28.961787	77.764844	Uttar Pradesh
69.	Jaibheem Nagar, Ward No. 5, Meerut, UdevriP	24.09503	83.0549	Uttar Pradesh

70.	Singrauli Super Thermal Power Plant, Singrauli	26.456382	80.320689	Uttar Pradesh
71.	Tejab Mill Campus, Anwarganj, Kanpur	26.2	80.54	Uttar Pradesh
72.	Mandoli & Seelampur, E- Waste site, Delhi	28.719159	77.314923	Delhi
73.	Ibrahimpur Village, Bhadarabad, Haridwar District, Uttarakhand	29.916654	78.071495	Uttarakhand
74.	Nibra Industrial Area, Howrah, West Bengal	22.603295	88.24852	West Bengal

Table S3. List of leading affiliations in the field of interest.

Affiliations	NoA	Rank based on NoA
University of Waterloo	39	1
University of Arizona	28	2
University of California	14	3
University of Florida	12	4
University of Tennessee	12	4
University of Toronto	12	4
Auburn University	11	7
Queen's University	11	7
Purdue University	9	9
Tufts University	9	9

Table S4. Effective diffusion coefficients estimated/used in the mathematical modeling studies related low permeability porous media.

Reference	Type of study	Aquitard thickness (m)	Effective diffusion coefficient, D^* (m^2/day)
[3]	Numerical modelling of field-scale study	10	6.1×10^{-5}
[4]	Analytical solutions for 2-D well controlled flow chamber experiments.	0.015	1.1×10^{-6}
[5]	Analytical model coupled with numerical transport simulator.	3 (<i>Dandy-Sale model problem</i>)	7.9×10^{-5} (<i>Dandy-Sale model problem</i>)
		5 (<i>Sand aquifer – thin clay layer problem</i>)	7.8×10^{-5} (<i>Sand aquifer – thin clay layer problem</i>)
		1.9×10^{-2}	2.6×10^{-5}
		5.6×10^{-1}	1.3×10^{-4}
		20	3.5×10^{-5}
[6] and references therein	Laboratory scale experiments and field study	40	3.5×10^{-5}
		130	2.2×10^{-5}
		130	2.7×10^{-6}
		220	2.1×10^{-6}
		200	3.0×10^{-6}
[7]	1-D analytical solutions for laboratory diffusion experiments.	0.03	1.5×10^{-6}
		0.07	3.4×10^{-5}
[8] and references therein	Computation of mass storage in hypothetical aquitard based on reported field data	5	9.8×10^{-8}
		5	1.8×10^{-6}
		5	1.2×10^{-5}
		5	2.8×10^{-5}

In the end, correlation analysis between distance and dispersivity is conducted to determine any relationship between longitudinal dispersivity and longitudinal distance. Also, correlation coefficient between transverse/lateral dispersivity and lateral/ transverse distance is calculated based on the data as shown in Table 6 which is compiled from major studies related to chlorinated solvents. It is observed that the $\alpha_{longitudinal}$ is positively correlated to longitudinal distance with 0.4894 correlation coefficient (R) as shown in Figure S1, whereas, strong positive correlation between $\alpha_{transverse}$ and transverse distance is obtained with $R = 0.7514$ and $P = 0.0003$ ($P < 0.05$ indicated that computed R is significant).

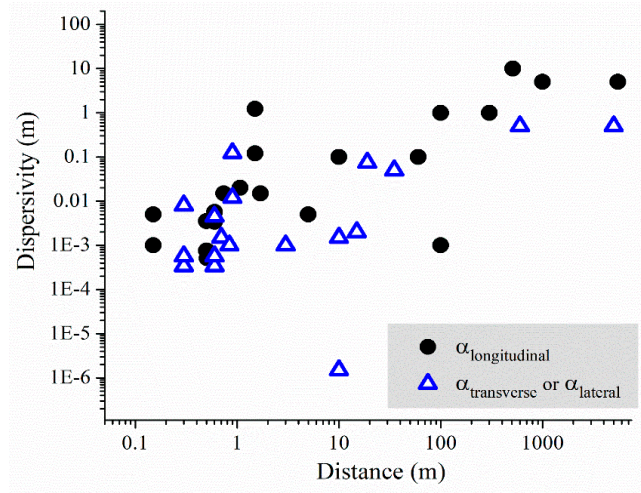


Figure S1. Variation of dispersivity with travel distance.

Table S5. Dispersion parameters used in various studies pertaining to DNAPL transport behavior in porous media.

Study Number	Reference	Type of study Numerical/ Field-scale/ Lab-scale	Longitudinal Distance (m)	Longitudinal dispersivity (m)	Transverse distance (m)	Transverse dispersivity (m)
R10	Clement et al. (2004b)	Experimental and numerical investigation for sand tank model (3-D)	1.7	0.015	0.6 <i>(horizontal y-direction)</i> 0.70 <i>(vertical z-direction)</i>	0.0045 <i>(horizontal y-direction)</i> 0.0015 <i>(vertical z-direction)</i>
R1	Clement et al. (2004a)	Modelling for hypothetical aquifer using 1-D approach.	510	10	-	-
R6	Chapman and Parker (2005)	Field study and Numerical modelling	300	1.0	15	0.002
R7	Chapman et al. (2012)	Laboratory-scale and Numerical Modelling	1.07	0.02	0.84	0.001
-	Erning et al. (2012)	2-D scenario modelling of DNAPL infiltration and spreading in laboratory scale experiment.	1.0 <i>(Length)</i>	Presented in terms of horizontal intrinsic permeability (m ²)	0.60 <i>(Height)</i>	Presented in terms of vertical intrinsic permeability (m ²)
R2	Vasudevan et al. (2014a)	Numerical study for soil column experiment (1-D).	0.15	0.001	-	-
-	Vasudevan et al. (2014b)	Multicomponent numerical modelling for saturated soil column (1-D).	0.15	0.001	-	-
R3	Berlin et al. (2015)	Numerical modelling for unsaturated subsurface system (1-D).	5	0.005	-	-
R11	Carey et al. (2015)	Modelled back-diffusion for field scale problem (2-D).	100 <i>(Length of aquifer)</i>	1 <i>(sand layer)</i> 0.001 <i>(clay layer)</i>	10 <i>(Thickness of aquifer)</i>	0.0015 <i>(vertical transverse direction- sand layer)</i> 1.5E-06 <i>(vertical transverse direction- clay layer)</i>

R8	Aydin-Sarikurt et al. (2016)	Numerical Modelling of TCE in the intermediate scale flushing tank (2-D).	0.74	0.015	0.30	0.008
R4	Knorr et al. (2016b)	Studied the fate of nitroaromatic compounds using experimental and mathematical modelling (1-D).	0.508	0.00051 to 0.00075	-	-
R5	Knorr et al. (2016a)	Analyzed transport behavior of non-reactive contaminant for saturated column experiments (1-D).	0.50	0.00076 to 0.00354	-	-
-	Vasudevan et al. (2016)	Saturated column was considered for investigation (1-D).	0.15	0.005	-	-
-	Falta and Wang (2017)	Simulated matrix diffusion for various type of contaminant transport problems (matrix diffusion in aquitard, Two-layer aquifer-aquitard solution).	- (Dandy-Sale model) 60 (fractured rock matrix diffusion problem)	- (Dandy-Sale model) 0.1 (fractured rock matrix diffusion problem)	3 (vertical - direction - Dandy-Sale problem) - (fractured rock matrix diffusion problem)	0.001 (vertical - direction - Dandy-Sale problem) - (fractured rock matrix diffusion problem)
R12	Guo and Brusseau (2017b, a)	Numerical modelling was carried out for hypothetical example and field scale data from Superfund site (3-D).	1000	5	600 (horizontal-transverse direction) 19 (vertical-transverse direction)	0.50 (horizontal-transverse direction) 0.075 (vertical-transverse direction)
-	Valsala and Govindarajan (2018b)	Mathematical modelling for fracture-rock matrix system (Pseudo 2-D, 1-D for fracture).	~100	1 0.1 to 10 (for sensitivity analysis)	-	-
R13	Guo et al. (2019a, b)	Numerical Modelling of TCE plume at field scale conditions (3-D).	~5500	5	5000 (horizontal y-direction) 20 to 35 (vertical)	0.5 (horizontal y-direction) 0.05

					<i>z-direction</i>	<i>(vertical z-direction)</i>
R9	Valsala and Govindarajan (2019)	Saturated aquifer conditions (2-D) were assumed for analysis.	10	0.1 0.001 to 0.1 <i>(for sensitivity analysis)</i>	5	0.01 0.001 to 0.1 <i>(for sensitivity analysis)</i>

Table S6. Laboratory-scale studies related to NAPL transport.

Reference	Setup type	Length (m)	Width or Thickness (m)	Height (m)
[27]	3-D physical laboratory-scale aquifer	1	0.75	1
[28]	3-D bench-scale homogeneous model aquifer	1.5	0.216	0.40
[29,30]	2-D laboratory scale tank	1	0.12	0.70
[31]	Saturated sand tank (3-D)	1	0.40	0.35
[32]	3-D sand aquifer	5.5	4.5	2.2
[33]	Column experimental setup	0.07	0.021 (<i>diameter</i>)	-
[34]	Laboratory scale study	1.5	0.02	0.60
[35]	2-D bench-scale tank study	0.773	0.011	0.14
[36]	2-D sandbox scale study	0.60	0.014	0.45
[17]	Laboratory-scale study	0.80	0.05	0.40
[37]	3-D box model	1	0.12	0.70
[38]	Laboratory-scale study (3-D)	0.60	0.30	0.60
[39]	Bench-scale tank study	1.40	0.70	0.50

Table S7. Source Mass Release Models used in the studies pertaining to dissolved DNAPL.

Reference	Source strength function/ Governing equation-based approach	Transport Processes	Critical Observations
[40,41]	$\frac{c_S(t)}{c_0} = \left(\frac{m(t)}{m_0}\right)^\Gamma$ $C_S(t) = \frac{c_0}{m_0^\Gamma} \left\{ \frac{-Q_S c_0}{\lambda_S m_0^\Gamma} + \left(m_0^{1-\Gamma} + \frac{Q_S c_0}{\lambda_S m_0^\Gamma} \right) e^{(\Gamma-1)\lambda_S t} \right\}^{\frac{\Gamma}{1-\Gamma}}$ $s(\mathbf{X}, t) = q_S C_S(t) \delta(x - x_{inj}) \mathbf{\Omega}(\mathbf{X} \in A_S)$	Flow and reactive transport model coupled with DNAPL mass release model.	<p>Mass depletion constant (Γ) > 1 correspond to finger dominated residual DNAPL.</p> <p>$\Gamma < 1$ correspond to site with DNAPL pools and lenses.</p> <p>Classical mass injection mode (CIM) and flux-weighted injection mode (FWIM) were compared.</p> <p>In CIM, PCE particles were uniformly injected within source area.</p> <p>Injection of particles for FWIM depend upon local cell fluxes.</p>
[32,42]	$R^{N,k} = k^{N,k} (C_{eq}^k - C^k)$	Solute transport model (SEAM3D) coupled to NAPL dissolution term	<p>First-order NAPL dissolution mass transfer term for species k was coupled with conventional contaminant transport equation.</p> <p>$\Gamma = 0.5 \Rightarrow$ Linear contaminant source depletion model</p> <p>$\Gamma = 1.0 \Rightarrow$ Exponential contaminant source depletion model</p>
[43,44]	$\frac{C_t}{C_0} = \left[1 + \frac{J_0}{M_0} (\Gamma - 1) t \right]^{\frac{\Gamma}{1-\Gamma}}, \Gamma > 0, \Gamma \neq 1$	1-D aquitard model with source strength function	<p>Concentration profiles in semi-infinite low-permeability zone were computed using 1-D analytical solutions.</p> <p>FN = forward diffusion with no-flux boundary present.</p>
[6]	Method of images based 1-D analytical solutions.	Diffusion between aquifers and a finite single aquitard system.	<p>BN = backward diffusion with no-flux boundary present.</p> <p>FF = forward diffusion with flux boundary.</p> <p>BF = backward diffusion with flux boundary.</p> <p>Analytical solution was developed for wide range of data for example, aquitard thickness</p>

			(L) and diffusion time (T) vary over 4 and 10 orders of magnitude.
[45]	$E^{an} = k^{an}(C_{eq}^a - C^a);$ $k^{an} = f_n(d_{50}, d_{10}, d_{60}, d_m, s_n, s_{ni}, D_m^a, Re')$	Three-dimensional contaminant transport model coupled with dissolution model	Rate-limited dissolution from an entrapped source zone was considered in the analysis.
[7]	$\frac{C_t}{C_0} = \left[\frac{\int_0^\infty C_t dt}{\int_0^\infty C_t dt} \right]^\Gamma = \left[\frac{M_t}{M_0} \right]^\Gamma$ <p>for $\Gamma = 1.0, C_t = C_0 \exp(-\beta t); \beta = \frac{J_0}{M_0}$</p> <p>1-D analytical solutions were used for forward and back diffusion with a no flux boundary Method of images was used.</p>	Diffusion between aquifer and thin clay aquitard region	Exponential source depletion model represented real field conditions for source strength behavior at contaminated sites.

Where C_t = time-dependent relative concentration of dissolved DNAPL [ML^{-3}]; C_0 = initial contaminant concentration [ML^{-3}] at the source zone plane; M_0 = initial mass [M] in the source zone; $J_0 = qAC_0$ = initial mass discharge rate [MT^{-1}] over the cross-sectional area, A [L^2] perpendicular to the Darcy flux, q [LT^{-1}]; Γ = dimensionless empirical parameter representing source strength function which depicts the effect of both flow field heterogeneity of aquifer and contaminant source distribution; t = difference between the time since the initial release and the arrival time of the contaminant at the down-gradient location [T]; E^{an} = interphase solute mass exchange between the nonaqueous and aqueous phases; k^{an} = Lumped mass transfer coefficient [T^{-1}]; C_{eq}^a = aqueous solubility of the DNAPL component which assumed to approximate the aqueous phase concentration of the component at the DNAPL and bulk aqueous interface [ML^{-3}]; C^a = solute mass concentration in aqueous phase [ML^{-3}]; d_m = diameter of a "medium-size" sand grain according to the ASTM particle size classification [L]; d_{50} = median grain size [L]; s_n = DNAPL saturation; s_{ni} = initial DNAPL saturation; D_m^a = aqueous phase molecular diffusion coefficient of the component [L^2T^{-1}]; Re' = modified Reynolds number; C^k = Aqueous phase concentration of species k [ML^{-3}]; C_{eq}^k = Compound-specific aqueous phase equilibrium concentration determined using Raoult's Law; $k^{N,k}$ = lumped NAPL mass transfer coefficient [T^{-1}]; $C_s(t)$ = averaged flux concentration of the dissolved phase DNAPL (PCE) leaving from the source zone [ML^{-3}]; $m(t)$ = mass of DNAPL remaining in the source zone [M]; m_0 = initial mass of DNAPL at the source zone [M]; Q_s = volumetric discharge rate of groundwater through source zone [L^3T^{-1}]; $\lambda_s = 1^{st}$ order degradation constant of PCE at the source zone [T^{-1}]; $\Omega(X \in A_s) = 1$ when $X \in A_s$ and 0 otherwise; $q_s = \frac{Q_s}{A_s}$

Table S8. Mathematical modelling-based studies emphasizing on transport of chlorinated solvent in the porous media.

Author and Year	Study interests	Methodology	Type of transport model	Spatial/ temporal domain scale	Key observations/ findings
[46]	Modelling of dissolution from fingers and pools of dense chlorinated solvent (PCE) in groundwater.	Analytical approach	Analytical solutions to 3-D advection - dispersion equation	Hypothetical 3-D	Superposition principle used to determine the overall contribution from fingers or pools of PCE.
[47]	Dissolution from DNAPLS in heterogeneous porous system.	Finite-difference method	Single and multicomponent DNAPLS pool	Synthetic example in 2-D	Steady flow conditions were assumed for saturated porous media. Degradation of DNAPL contaminant into daughter species was not considered. NAPL dissolution was assumed to occur in the aquifer region only. Sorption term was neglected in the study.
[9]	Dissolution pattern of entrapped DNAPL in saturated sand tank.	Integrated NAPL dissolution and conventional solute transport model	3-dimensional solute transport (RT3D) code	3-dimensional sand tank	Aqueous phase solubility level of the NAPL, dissolution mass transfer related factors were identified as critical parameters.
[10]	Modelled (Tetrachloroethene) DNAPL-dissolution, rate-limited sorption, and biodegradation.	Integrated model approach including dissolution, rate-limited sorption, and biodegradation	3-dimensional solute transport (RT3D) reaction package	Hypothetical 3-D case study	Combined effect of physical, chemical and biological reactive processes on contaminant transport was considered. Mass-transfer process showed non-linear behavior for various sorption rates.
[3]	Investigated plume persistence in the aquitard after removal/ isolation of DNAPL (TCE) source	Finite element based numerical modelling	HydroGeo-sphere	Field-scale (2-D vertical cross-sectional plane)	Advection and dispersion were assumed for the aquifer region, however only diffusion of TCE was considered in the underlying aquitard layer. Step declining source term performed better as compared to constant source term.

[48,49]	Modelling of dissolved phase contaminant plumes of BTEX and chlorinated ethenes in heterogeneous aquifers.	Semi-analytical approach	Coupled flux-tube (FT) and Mixed Instantaneous and Kinetics Superposition Sequence (MIKSS) based approach	Theoretical and field study	Effect of transverse horizontal dispersion was neglected for field-scale study. FT-MIKSS based approach was 100 to 1000 times computationally faster in comparison to numerical models (RT3D, PHT3D, PHAST) for various tested cases. Faster parameter fitting was observed for field studies.
[50]	Computed contaminant mass stored in aquitard due to DNAPL source depletion.	Analytical approach	Analytical solution to 1-D diffusion equation coupled with source depletion model (SDM)	Hypothetical example	Power law SDM was used to mimic the source zone dissolution and used as boundary condition in the contaminant transport equation. Impact of source zone architecture and source to aquitard mass transfer coefficient was assessed using parameters like contaminant mass in aquitard, magnitude and longevity of back-diffusion flux.
[11]	Applicability of finite element and finite difference-based model was assessed to simulate transport behavior in low-permeability zone.	Numerical Model	FEFLOW, MODFLOW-MT3DMS, HydroGeosphere	Sand tank experiment	Numerical simulations were conducted at high resolution to compute diffusion flux into/out of low permeability zones.
[12]	Investigated the transport behavior of DNAPL (TCE) for various flow velocities and various subsurface geometries.	Multiphase Modelling	TMVOC coupled with Petrasim	Laboratory scale experiment (2D scenario Modelling)	DNAPL source zone was found as highly sensitive to groundwater flow velocity in comparison to the geometrical formation of porous media.

[51]	Simulated complex network reactions in heterogeneous porous media.	Random Walk Particle Tracking Method	Multispecies reactive transport modelling	Synthetic example in 3-D space	Simulated the reductive dechlorination of the PCE in spatially heterogeneous system. Linear sorption isotherm was assumed, and biodegradation was neglected for sorbed phase solute concentration.
[52]	Analytical modelling tool was developed for representing contaminant source history at the low permeability zones.	Spreadsheet based analytical modelling tool. Depth-wise soil concentration data was used.	1-D diffusion equation	Field-scale data	Coupled source history tool with contaminant transport model. Modified model was applied to four different sites contaminated with chlorinated ethenes.
[16]	Numerical model was developed to simulate diffusion-dominated processes at field-scale conditions.	Numerical Model	3-D multispecies transport model coupled with local 1-D domain model	Field-scale modelling	In situ remediation MT3DMS model involving local 1-D domain model was developed to simulate diffusive flux from silt/clay layers at field-scale conditions. Remediation timeframes were dominantly governed by transverse vertical dispersivity, input parameters of back-diffusion model, and length of silt/clay layers.
[17]	Investigated the impact of cosolvent flushing on the solubilization and mobilization of TCE.	Numerical Modelling	Multiphase flow modelling program UTCHEM - 9.0	Intermediate-scale flushing tank experiment	Analyzed the impact of cosolvent content, injection pattern, and velocity of flushing solution on the mass transfer rate.
[20]	Investigated dissolution mass-transfer of entrapped hydrocarbon in saturated sub-surface system.	Dual-domain based approach (Mobile-immobile method)	Single species (toluene)	15 cm laboratory-scale soil column (1D study)	Constant dispersivity function was used in the governing transport equation.
[5]	Semi-analytical model was developed to	Semi-analytical approach	1-D diffusion equation coupled with 3-D	Two-layer aquitard-aquifer, fracture-	Matrix diffusion fluxes from low permeability materials were incorporated as concentration-dependent source/sink terms

	simulate matrix diffusion in porous media.		contaminant transport equation	matrix system (published studies)	in the conventional numerical transport model. Model performed well during loading period in comparison to back-diffusion period. Relationship between contaminant mass discharge (CMDR) and mass removal (MR) was used as index to characterize the effects of various factors and scenarios.
[21,22]	Effects of well field configuration and permeability heterogeneity on the plume persistence and contaminant mass removal were studied.	3-D Finite difference method	MODFLOW, MT3DMS, Random walk-based method (RWheat)	Hypothetical example, Field-scale data of Superfund site	Pump and treat mass removal efficiency was observed as dominated by well field configuration for homogeneous systems. Non ideal mass removal behavior observed for the layered porous systems was contributed by well field configuration and diffusive mass transfer from low permeability zone. Aquifer contaminant data from mature sites was described well by using analytical solution in which source zone and back-diffusion term had been considered. Back diffusion term solely represented field data from sites which had been isolated from contaminant source.
[43]	Analyzed aquitard concentration data from field sites and predicted long-term contaminant plume behavior.	1-D analytical model for single aquifer-aquitard system	Analytical solution integrated with DNAPL source dissolution term	Field-scale data (1-D diffusion equation)	Dynamic aquifer-aquitard boundary conditions incorporated in analytical solutions were successful in modelling concentration profiles in aquitards and flux-averaged solute concentrations in surrounding aquifers.
[6]	Analytical solutions were used to study solute diffusion in porous system comprising of finite aquitard sandwiched between aquifer regions.	1-D diffusion model	Analytical solution to 1-D diffusion equation	Laboratory experiment, field site data	Non-equilibrium sorption, matrix diffusion, and aerobic biodegradation were
[23]	Investigated the transport of dissolved	Finite-difference method	Transport equations were	Pseudo 2-D space	

	Benzene, Toluene, Ethylbenzene, and Xylene (BTEX) in fractured-matrix system.		related to BTEX constituents along with dissolved oxygen and biomass	Hypothetical case study	considered to study the fate and transport of dissolved BTEX plume in fracture-matrix system. Sorption and biodegradation reactions significantly affected the mobility of dissolved BTEX during early travel time. Integration of time-dependent dissolution from an entrapped source zone with solute transport model. Entrapped DNAPL source zones were observed as persistent source of low concentration plume and unidentifiable from sorbed and immobile dissolved mass sources.
[45]	Investigated the comprehensive effect of dissolution, sorption, and diffusion on plume persistence in heterogeneous porous media.	Multiphase Modelling	Modified version of MT3DMS	Hypothetical site (2-D and 3-D)	2-D simulations were not accurate and emphasized the requirement of 3-D modelling for the nonideal sorption case. Study was limited to short-travel distance (10 m within DNAPL source zone).
[24,25]	Implemented geostatistical approach coupled with numerical contaminant transport to simulate pump and treat operations.	Random-field generator, Finite difference based Ground-water flow and solute transport model, Random walk based method	T-PROGS, MODFLOW, MT3DMS, Random walk-based method (RWheat)	Field-scale data from Tucson International Airport Area (TIAA) federal Superfund site	Markov chain based stochastic method was implemented to generate random distribution of heterogeneity. Compared MT3DMS and RWheat for field scale numerical modelling. RWheat was observed as computationally efficient than MT3DMS.
[7]	Evaluated the effects of source depletion and diffusion into/out of aquitard on the dissolved phase plume persistence.	Analytical solution using method of images	1-D diffusion equation with source depletion model	Laboratory diffusion experiment	Solute mass accumulation in the aquitard was observed for longer time span for the case of lower rates of source depletion.

[8]	Impact of cracks on the TCE mass accumulation in the aquitard region was assessed.	Analytical approach	Equation pertaining to diffusion of dissolved phase TCE	3-D Hypothetical aquitard of clay layer	Mass accumulation in aquitard after 30 years was calculated for three scenarios i.e. (i) diffusion without cracks, (ii) advective flux movement into cracks and then diffusion from cracks, and (iii) TCE present in the cracks in the aquitard.
-----	--	---------------------	---	---	--

Table S9. List of Top 10 documents in the field of DNAPL transport in the aquifer systems.

First author of the article	Focus of the article	TCi	TCi per Year	Normalized TCi	Reference
O'Carroll D.	Review on background knowledge, numerical tools, and technology related to reactions of nano zero valent iron (nZVI) with chlorinated solvents and metals in the subsurface remediation operations. Challenges encountered during implementation of nZVI at field-scale conditions were discussed.	606	60.60	8.75	O'Carroll et al. (2013)
Moody C.A.	A critical review on the properties of fluorinated surfactants and their impact on co-contaminant (DNAPL) transport and biodegradation in the subsurface.	441	19.17	6.31	Moody and Field (2000)
Saleh N.	Investigation of effects of different surface modifications on transportability and dispersion stability of nanoiron in water-saturated porous system. Study on effects of surface modifications on the reactivity of nanoiron with TCE.	383	23.94	8.27	Saleh et al. (2007)
He F.	Investigation of long-term effectiveness of carboxymethyl cellulose (CMC) stabilized nano particles for <i>in-situ</i> degradation of chlorinated solvents at pilot-scale subsurface conditions.	333	25.62	4.97	He et al. (2010)
Yan W.	A review study on recent advancements in nZVI for remediation of groundwater system. Summarize the critical findings obtained from field experiences.	298	29.80	4.31	Yan et al. (2013)
He F.	Study on transport of carboxymethyl cellulose (CMC) stabilized ZVI nano particles in saturated porous media through column experiments and numerical modelling. Simulation of observed data via classical filtration theory and modified convection-dispersion equation.	221	15.79	5.15	He et al. (2009)
Kim H.	A study on degradation of TCE by nZVI in alginate bead.	180	13.85	2.68	Kim et al. (2010)
Sung Y.	Isolation and characterization of acetotrophic PCE dechlorinators and comparison with <i>Desulfuromonas chloroethenica</i>	177	8.85	5.01	Sung et al. (2003)

	Investigation of various physiological properties affecting bioremediation processes.				
Liang C.	Study of transport of persulfate and TCE in column filled with glass beads and sandy soil simulating <i>in situ</i> chemical oxidation remediation of TCE.	170	11.33	2.29	Liang et al. (2008)
Aulenta F.	Development of BEARD: bio-electrochemically assisted reductive dechlorination process-based proof of concept for <i>in-situ</i> bioremediation of chlorinated-solvent-contaminated groundwater.	165	10.31	3.56	Aulenta et al. (2007)

Table S10. List of Most Influential Authors in the Research Field based on TCi main criteria.

Author	TCi	Rank based on TCi	NoA	Rank based on NoA	PSY
He F.	718	1	5	3	2009
Zhao D.	659	2	4	4	2009
Boparai H.	606	3	1	6	2013
Kocur C.	606	3	1	6	2013
Krol M.	606	3	1	6	2013
O'carroll D.	606	3	1	6	2013
Sleep B.	606	3	1	6	2013
Cherry J.A.	503	8	13	1	1992
Parker B.L.	502	9	13	1	2004
Lowry G.V.	487	10	4	4	2007

Table S11 List of Most Influential Authors in the Research Field based on NoA main criteria.

Element	NoA	Rank based on NoA	TCi	Rank based on TCi	PSY
Cherry J.A.	13	1	503	1	1992
Parker B.L.	13	1	502	2	2004
Abriola L.M.	11	3	376	3	1998
Brusseau M.L.	11	3	281	6	1999
Annable M.D.	10	5	336	4	1998
Clement T.P.	8	6	325	5	2000
Rivett M.O.	8	6	251	8	1994
Sudicky E.A.	8	6	242	9	1996
Chapman S.W.	7	9	272	7	2004
Pennell K.D.	7	9	233	10	2002

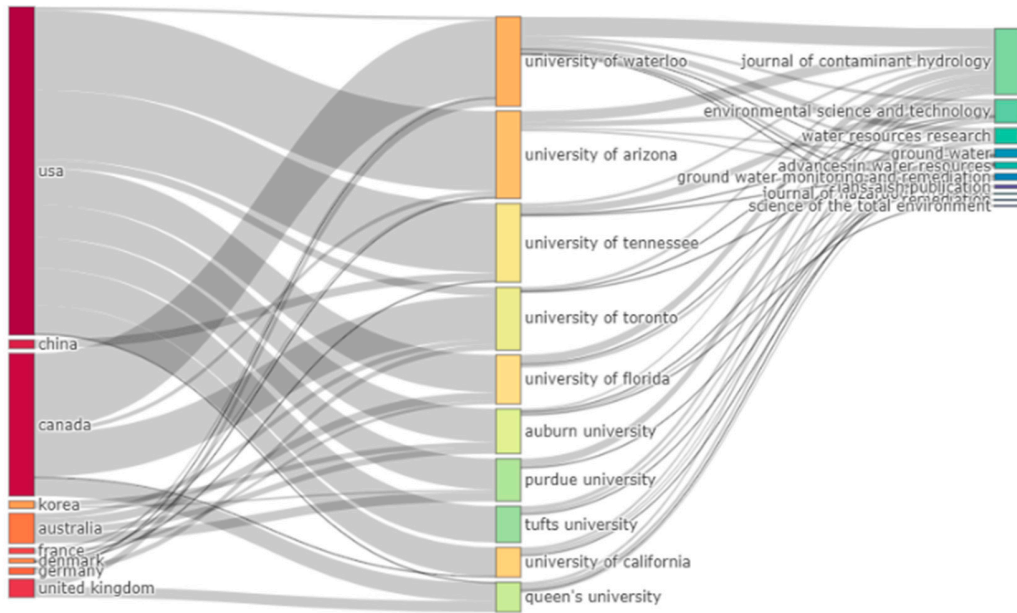


Figure S2. Three-Field Plot of Author's Country (Left), Affiliation (Middle), and Source - Journal (Right).

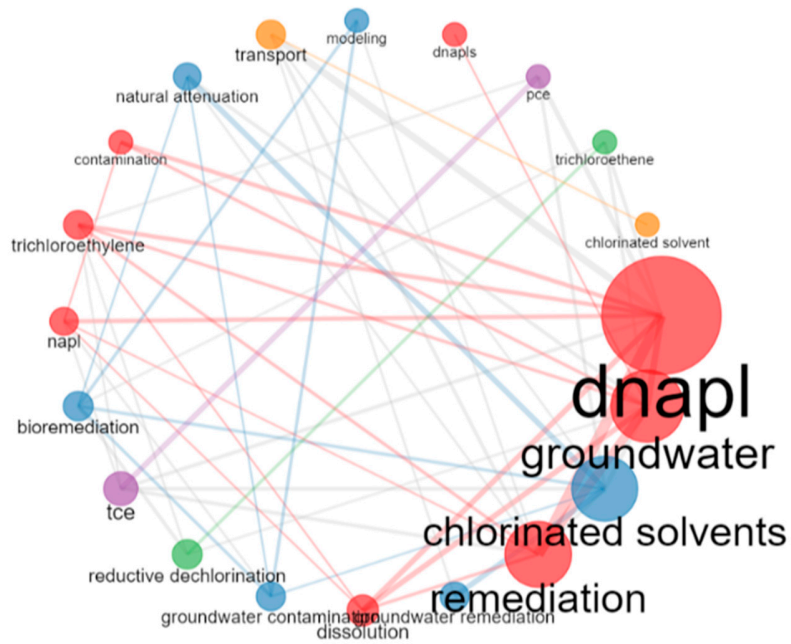


Figure S3. Co-occurrence network of Top 20 most influential "Author's Keywords" as per Scopus Database from 1990-2022.

S1. Network visualization of cited references

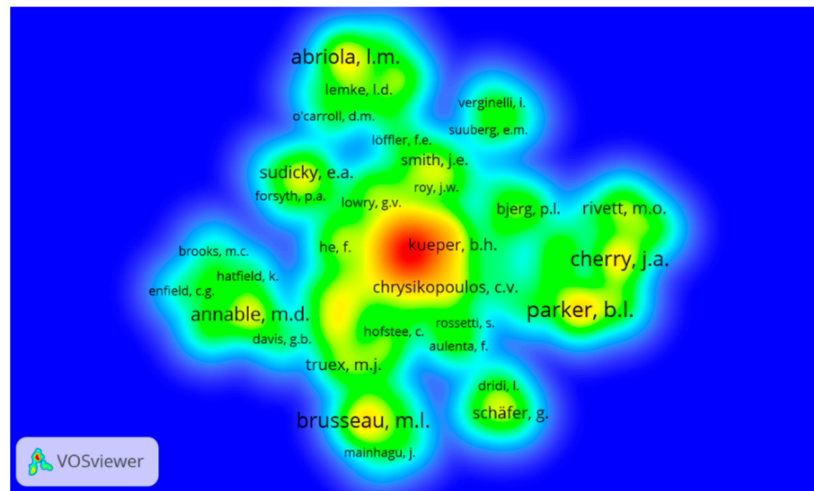


Figure S4. Co-citation network visualization of “cited references” obtained via VOSviewer.

The co-citation network of cited references of DNAPL transport research field from Scopus database was generated via VOSviewer, with “Lin/Log normalization” method performing well as shown in Figure S4. The label on the node shows the brief details of first author or first and second author. It is observed that only 92 authors out of 1063 authors had a minimum number of 3 documents in the Scopus database. Parker, B.L. and Cherry, J.A. were observed on the right side of network and had a strong connection, whereas Brusseau, M.L. was found in the bottom portion of network (Figure S4). The network was found to be scattered, and references were clustered in small groups. The cluster in the center of the network was observed to be led by Kueper, B.H., and Chrysiopoulos, C.V. and has a wide loose network of connections with references named He, F., Lowry, G.V., Truxex, M.J., and Rossetti, S. The left-side cluster was found to be led by Annable, M.D. and has a loose network of connections with references named Hatfield, K., Brooks, M.D., Davis, G.B., and Enfield, C.G.

S2. Findings of bibliometric analysis

S2.1 Characterization of published articles

The list of top 10 most influential articles is shown in Table S9 of supplementary information. It is observed that all of top ten articles were cited more than 150 times, and article by O'Carroll et al. (2013) ranked in the first position with 606 *TCi* and 60.60 *TCi* per year. The highest-ranked article by O'Carroll et al. (2013) discussed the background knowledge and numerical tools pertaining to reactions of nano zero-valent iron (nZVI) with chlorinated solvents and metals during remediation operations and further discussed the limitations at field-scale conditions. The second rank article based on the *TCi* is oldest article among top articles; however, article ranked 5th based on *TCi* per year [54]. The article critically reviewed the fate, transport, and impacts of aqueous film forming foam (AFFF) agents and fluorinated surfactants on co-contaminant (DNAPL) transport and biodegradation in the subsurface [54]. The research article by Saleh et al. (2007), ranked in 3rd and 4th position based on *TCi* and *TCi* per year criterion, investigated the effects of surface modifications on the nano iron transport and reaction dynamics with TCE. The fourth and sixth-ranked articles, based on the *TCi* parameter, studied the impact and transport dynamics of carboxymethyl cellulose (CMC) stabilized nanoparticles at column- and pilot-scale conditions via numerical modelling and experiments [56,58]. A detailed description of various parameters of top ten influential articles in DNAPL research field is shown in Table S9 of supplementary information.

S2.2 Characterization of publication sources

The most dominant sources or journals based on the *TCi*, and NoA are shown in Table S12. *Journal of Contaminant Hydrology* ranked first in the list based on *TCi* and NoA published from 1990 through 2022. *Environmental Science and Technology* and *Water Resources Research* ranked second and third with 2127 and 971 *TCi*. *Advances in Water Resources* ranked in fourth position on the basis of *TCi*; however, it ranked in fifth position based on NoA. On the basis of NoA, *Groundwater* and *Environmental Engineering Science* ranked in fifth and sixth positions based on the *TCi* value. *Chemosphere* was observed at tenth position based on the *TCi*, while *Environmental Sciences: Processes and Impacts* ranked in tenth position on the basis of NoA. It was found that all the top five journals received at least 750 citations from 1990 to 2022. It can be stated that the top three publishing journals in DNAPL transport research field also received the highest number of citations.

Table S12. List of Top 10 Journals (Sources).

Element	<i>TCi</i>	Rank based on <i>TCi</i>	NoA	Rank based on NoA
Journal of Contaminant Hydrology	3574	1	106	1
Environmental Science and Technology	2127	2	35	2
Water Resources Research	971	3	20	3
Advances in Water Resources	842	4	13	5
Groundwater	786	5	16	4
Environmental Engineering Science	494	6	5	7
Water Research	487	7	4	9
Journal of Hazardous Materials	446	8	12	6
Environmental Sciences: Processes and Impacts	298	9	1	10
Chemosphere	252	10	5	7

S2.3 Contribution of authors

The author's productivity and impact of influential authors in the DNAPL transport research field were shown on the basis of total citations (TCi) and a number of articles (NoA) publications statistics (Table S10). He F., with a 718 TCi value, was ranked in the first position based on the Scopus® database from 1990 through 2022; however, author was ranked in the third position based on the number of articles published. Cherry J.A., Adjunct Professor, University of Guelph, and Distinguished Professor Emeritus, University of Waterloo, published a total of 13 articles related to DNAPL transport modelling and received a total citation of 503 for those published articles, ranked in the first position on the basis of NoA (Table S11 of supplementary information). Similarly, author Parker B.L., Director, Morwick G360 Groundwater Research Institute, belongs to the School of Engineering, University of Guelph, ranked in the first position on the basis of NoA, received a total of 502 citations, and has published 13 articles. It was found that the top two authors (Parker B.L. and Cherry J.A.), worked together on several articles on DNAPL transport in collaboration. It was observed that the authors who had published at least ten articles had received citations higher than 250 (Table S11).

S2.4 Co-occurrence analysis and content analysis

Sankey diagrams (three-field plots) are used to display the interconnections between different attributes of the research database [73,74]. The essential elements are presented by rectangular diagrams with different colors. The sum of flux weights is conserved at each node of the Sankey diagram. The number of communications between multiple components of three-field plots directly depends upon the height of the rectangle [73]. Figure S2 shows the relationship of the author's country with leading affiliations and top journals publishing papers on DNAPL transport research field. The strong connection and dominance of USA and Canada were observed from Sankey diagram. It is observed that most of the authors from USA and Canada published articles in the journals with highest to lowest priority as in order as Journal of Contaminant Hydrology, Environmental Science and Technology, Water Resources Research, and Groundwater.

The co-occurrence network of author's keywords in DNAPL transport research field, considering 20 nodes, is shown in Figure S3 of supplementary information. A circle was used as a networking layout, and InfoMap was used as a clustering algorithm. An association method was kept as a normalization method. The size of the node depicts the node's strength, and connection strength is depicted by line thickness. It is observed that the "dnapl" dominates the author's keywords list, followed by "groundwater", "chlorinated solvents", and "remediation". The "dnapl" node (shown in red) has a strong link with the "dissolution", "napl", "contamination", and "trichloroethylene" nodes, whereas the "chlorinated solvents" node has a significant connection with "natural attenuation" and "bioremediation" nodes. Also, a small-sized node such as "pce" has a strong connection with node "tce" which can be assumed as a reasonable result because tetrachloroethylene is converted into trichloroethylene under reductive dechlorination process. In addition, nodes such as "modeling", "transport", "reductive dechlorination", and "natural attenuation" occurred in the network, too, indicating the prominence of such authors' keywords in the DNAPL transport research field.

S2.5 Thematic map analysis

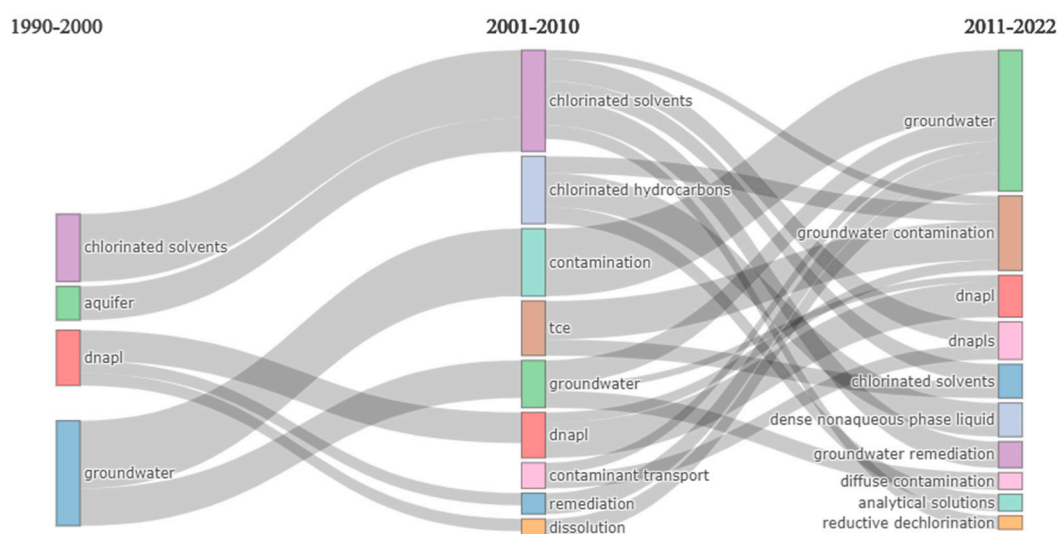


Figure S5. Evolution of thematic map with time based on “author’s keywords”.

Thematic evolution is analyzed in past studies using a three-field plot, which depicts the evolution and connection of different themes with time [75,76]. The theme is represented by a rectangular box, and size of the box denotes how frequently the theme occurred in the database of a research field. Thematic evolution maps were developed based on the author’s keywords searching criteria between three-time levels from 1990-2000 to 2001-2010 to 2011-2022. Figure S5 shows thematic evolution of author’s keywords in the DNAPL transport research field. It is observed that the “chlorinated solvents”, “aquifer”, “dnapl”, and “groundwater” keywords dominated the DNAPL transport research field from 1990-2000. Further, from 2001 to 2010, new keywords such as “contamination”, “tce”, “remediation”, “dissolution”, “chlorinated hydrocarbons”, and “contaminant transport” appeared in the Sankey diagram. However, in recent years, “groundwater”, “groundwater contamination”, and “dnapl” dominated the research field in time span 2011-2022. Also, authors’ keywords such as “diffuse contamination”, “reductive dechlorination”, and “analytical solutions” appeared in the timespan 2011-2022, depicting the development of field towards development of semi-analytical and/or analytical solutions.

References

1. CPCB *State Wise List of Contaminated Sites*; Central Pollution Control Board, Waste Management Division-I, 2022;
2. Gupta, P.K. Pollution Load on Indian Soil-Water Systems and Associated Health Hazards: A Review. *J. Environ. Eng.* **2020**, *146*, 03120004, doi:10.1061/(ASCE)EE.1943-7870.0001693.
3. Chapman, S.W.; Parker, B.L. Plume Persistence Due to Aquitard Back Diffusion Following Dense Nonaqueous Phase Liquid Source Removal or Isolation. *Water Resour. Res.* **2005**, *41*, 1–16, doi:10.1029/2005WR004224.
4. Yang, M.; Annable, M.D.; Jawitz, J.W. Back Diffusion from Thin Low Permeability Zones. *Environ. Sci. Technol.* **2015**, *49*, 415–422, doi:10.1021/es5045634.
5. Falta, R.W.; Wang, W. A Semi-Analytical Method for Simulating Matrix Diffusion in Numerical Transport Models. *J. Contam. Hydrol.* **2017**, *197*, 39–49, doi:10.1016/j.jconhyd.2016.12.007.
6. Yang, M.; Annable, M.D.; Jawitz, J.W. Forward and Back Diffusion through Argillaceous Formations. *Water Resour. Res.* **2017**, *53*, 4514–4523, doi:10.1002/2016WR019874.
7. Yang, M.; McCurley, K.L.; Annable, M.D.; Jawitz, J.W. Diffusion of Solutes from Depleting Sources into and out

- of Finite Low-Permeability Zones. *J. Contam. Hydrol.* **2019**, *221*, 127–134, doi:10.1016/j.jconhyd.2019.01.005.
8. Ayral-Çınar, D.; Demond, A.H. Accumulation of DNAPL Waste in Subsurface Clayey Lenses and Layers. *J. Contam. Hydrol.* **2020**, *229*, 103579, doi:10.1016/j.jconhyd.2019.103579.
 9. Clement, T.P.; Kim, Y.-C.; Gautam, T.R.; Lee, K.-K. Experimental and Numerical Investigation of DNAPL Dissolution Processes in a Laboratory Aquifer Model. *Ground Water Monit. Remediat.* **2004**, *24*, 88–96, doi:10.1111/j.1745-6592.2004.tb01306.x.
 10. Clement, T.P.; Gautam, T.R.; Lee, K. kun; Truex, M.J.; Davis, G.B. Modeling of DNAPL-Dissolution, Rate-Limited Sorption and Biodegradation Reactions in Groundwater Systems. *Bioremediat. J.* **2004**, *8*, 47–64, doi:10.1080/10889860490453177.
 11. Chapman, S.W.; Parker, B.L.; Sale, T.C.; Doner, L.A. Testing High Resolution Numerical Models for Analysis of Contaminant Storage and Release from Low Permeability Zones. *J. Contam. Hydrol.* **2012**, *136–137*, 106–116, doi:10.1016/j.jconhyd.2012.04.006.
 12. Erning, K.; Grandel, S.; Dahmke, A.; Schäfer, D. Simulation of DNAPL Infiltration and Spreading Behaviour in the Saturated Zone at Varying Flow Velocities and Alternating Subsurface Geometries. *Environ. Earth Sci.* **2012**, *65*, 1119–1131, doi:10.1007/s12665-011-1361-9.
 13. Vasudevan, M.; Suresh Kumar, G.; Nambi, I.M. Numerical Study on Kinetic/Equilibrium Behaviour of Dissolution of Toluene under Variable Subsurface Conditions. *Eur. J. Environ. Civ. Eng.* **2014**, *18*, 1070–1093, doi:10.1080/19648189.2014.922902.
 14. Vasudevan, M.; Suresh Kumar, G.; Nambi, I.M. Numerical Modelling of Multicomponent LNAPL Dissolution Kinetics at Residual Saturation in a Saturated Subsurface System. *Sadhana* **2014**, *39*, 1387–1408, doi:10.1007/s12046-014-0282-1.
 15. Berlin, M.; Vasudevan, M.; Kumar, G.S.; Nambi, I.M. Numerical Modelling on Fate and Transport of Petroleum Hydrocarbons in an Unsaturated Subsurface System for Varying Source Scenario. *J. Earth Syst. Sci.* **2015**, *124*, 655–674, doi:10.1007/s12040-015-0562-0.
 16. Carey, G.R.; Chapman, S.W.; Parker, B.L.; McGregor, R. Application of an Adapted Version of MT3DMS for Modeling Back-Diffusion Remediation Timeframes. *Remediat. J.* **2015**, *25*, 55–79, doi:10.1002/rem.21440.
 17. Aydin-Sarikurt, D.; Dokou, Z.; Copty, N.K.; Karatzas, G.P. Experimental Investigation and Numerical Modeling of Enhanced DNAPL Solubilization in Saturated Porous Media. *Water, Air, Soil Pollut.* **2016**, *227*, 441, doi:10.1007/s11270-016-3136-0.
 18. Knorr, B.; Maloszewski, P.; Stumpp, C. Quantifying the Impact of Immobile Water Regions on the Fate of Nitroaromatic Compounds in Dual-Porosity Media. *J. Contam. Hydrol.* **2016**, *191*, 44–53, doi:10.1016/j.jconhyd.2016.05.002.
 19. Knorr, B.; Maloszewski, P.; Krämer, F.; Stumpp, C. Diffusive Mass Exchange of Non-Reactive Substances in Dual-Porosity Porous Systems - Column Experiments under Saturated Conditions. *Hydrol. Process.* **2016**, *30*, 914–926, doi:10.1002/hyp.10620.
 20. Vasudevan, M.; Suresh Kumar, G.; Nambi, I.M. Numerical Modelling on Rate-Limited Dissolution Mass Transfer of Entrapped Petroleum Hydrocarbons in a Saturated Sub-Surface System. *ISH J. Hydraul. Eng.* **2016**, *22*, 3–15, doi:10.1080/09715010.2015.1043596.
 21. Guo, Z.; Brusseau, M.L. The Impact of Well-Field Configuration on Contaminant Mass Removal and Plume Persistence for Homogeneous versus Layered Systems. *Hydrol. Process.* **2017**, *31*, 4748–4756, doi:10.1002/hyp.11393.
 22. Guo, Z.; Brusseau, M.L. The Impact of Well-Field Configuration and Permeability Heterogeneity on

- Contaminant Mass Removal and Plume Persistence. *J. Hazard. Mater.* **2017**, *333*, 109–115, doi:10.1016/j.jhazmat.2017.03.012.
23. Valsala, R.; Govindarajan, S.K. Mathematical Modeling on Mobility and Spreading of BTEX in a Discretely Fractured Aquifer System Under the Coupled Effect of Dissolution, Sorption, and Biodegradation. *Transp. Porous Media* **2018**, *123*, 421–452, doi:10.1007/s11242-018-1049-7.
24. Guo, Z.; Brusseau, M.L.; Fogg, G.E. Determining the Long-Term Operational Performance of Pump and Treat and the Possibility of Closure for a Large TCE Plume. *J. Hazard. Mater.* **2019**, *365*, 796–803, doi:10.1016/j.jhazmat.2018.11.057.
25. Guo, Z.; Fogg, G.E.; Brusseau, M.L.; LaBolle, E.M.; Lopez, J. Modeling Groundwater Contaminant Transport in the Presence of Large Heterogeneity: A Case Study Comparing MT3D and RWHEAT. *Hydrogeol. J.* **2019**, *27*, 1363–1371, doi:10.1007/s10040-019-01938-9.
26. Valsala, R.; Govindarajan, S.K. Co-Colloidal BTEX and Microbial Transport in a Saturated Porous System: Numerical Modeling and Sensitivity Analysis. *Transp. Porous Media* **2019**, *127*, 269–294, doi:10.1007/s11242-018-1191-2.
27. Anderson, M.R.; Johnson, R.L.; Pankow, J.F. Dissolution of Dense Chlorinated Solvents into Ground Water: 1. Dissolution from a Well-Defined Residual Source. *Ground Water* **1992**, *30*, 250–256, doi:10.1111/j.1745-6584.1992.tb01797.x.
28. Lee, K.; Chrysikopoulos, C. Dissolution of a Multicomponent DNAPL Pool in an Experimental Aquifer. *J. Hazard. Mater.* **2006**, *128*, 218–226, doi:10.1016/j.jhazmat.2005.08.005.
29. Luciano, A.; Viotti, P.; Papini, M.P. Laboratory Investigation of DNAPL Migration in Porous Media. *J. Hazard. Mater.* **2010**, *176*, 1006–1017, doi:10.1016/j.jhazmat.2009.11.141.
30. Luciano, A.; Mancini, G.; Torretta, V.; Viotti, P. An Empirical Model for the Evaluation of the Dissolution Rate from a DNAPL-Contaminated Area. *Environ. Sci. Pollut. Res.* **2018**, *25*, 33992–34004, doi:10.1007/s11356-018-3193-6.
31. Sulaymon, A.H.; Gzar, H.A. Experimental Investigation and Numerical Modeling of Light Nonaqueous Phase Liquid Dissolution and Transport in a Saturated Zone of the Soil. *J. Hazard. Mater.* **2011**, *186*, 1601–1614, doi:10.1016/j.jhazmat.2010.12.035.
32. Mobile, M.A.; Widdowson, M.A.; Gallagher, D.L. Multicomponent NAPL Source Dissolution: Evaluation of Mass-Transfer Coefficients. *Environ. Sci. Technol.* **2012**, *46*, 10047–10054, doi:10.1021/es301076p.
33. Brusseau, M.L.; Russo, A.E.; Schnaar, G. Nonideal Transport of Contaminants in Heterogeneous Porous Media: 9 – Impact of Contact Time on Desorption and Elution Tailing. *Chemosphere* **2012**, *89*, 287–292, doi:10.1016/j.chemosphere.2012.04.038.
34. Maruo, T.; Ryuichiltoi; Tanaka, T.; Iwasaki, M.; Oishi, H. Laboratory Experiment of Tracer Test with Vertical Two-Dimensional Porous Media. *Procedia Earth Planet. Sci.* **2013**, *6*, 121–130, doi:10.1016/j.proeps.2013.01.017.
35. Ballarini, E.; Bauer, S.; Eberhardt, C.; Beyer, C. Evaluation of the Role of Heterogeneities on Transverse Mixing in Bench-Scale Tank Experiments by Numerical Modeling. *Groundwater* **2014**, *52*, 368–377, doi:10.1111/gwat.12066.
36. Zheng, F.; Gao, Y.; Sun, Y.; Shi, X.; Xu, H.; Wu, J. Influence of Flow Velocity and Spatial Heterogeneity on DNAPL Migration in Porous Media: Insights from Laboratory Experiments and Numerical Modelling. *Hydrogeol. J.* **2015**, *23*, 1703–1718, doi:10.1007/s10040-015-1314-6.
37. Tatti, F.; Petrangeli Papini, M.; Torretta, V.; Mancini, G.; Boni, M.R.; Viotti, P. Experimental and Numerical Evaluation of Groundwater Circulation Wells as a Remediation Technology for Persistent, Low Permeability

- Contaminant Source Zones. *J. Contam. Hydrol.* **2019**, *222*, 89–100, doi:10.1016/j.jconhyd.2019.03.001.
38. Gupta, P.K.; Yadav, B.K. Three-Dimensional Laboratory Experiments on Fate and Transport of LNAPL under Varying Groundwater Flow Conditions. *J. Environ. Eng.* **2020**, *146*, 04020010, doi:10.1061/(ASCE)EE.1943-7870.0001672.
39. Vaezihir, A.; Bayanlou, M.B.; Ahmadnezhad, Z.; Barzegari, G. Remediation of BTEX Plume in a Continuous Flow Model Using Zeolite-PRB. *J. Contam. Hydrol.* **2020**, *230*, 103604, doi:10.1016/j.jconhyd.2020.103604.
40. Henri, C. V.; Fernández-García, D.; de Barros, F.P.J. Probabilistic Human Health Risk Assessment of Degradation-Related Chemical Mixtures in Heterogeneous Aquifers: Risk Statistics, Hot Spots, and Preferential Channels. *Water Resour. Res.* **2015**, *51*, 4086–4108, doi:10.1002/2014WR016717.
41. Henri, C. V.; Fernández-García, D.; de Barros, F.P.J. Assessing the Joint Impact of DNAPL Source-Zone Behavior and Degradation Products on the Probabilistic Characterization of Human Health Risk. *Adv. Water Resour.* **2016**, *88*, 124–138, doi:10.1016/j.advwatres.2015.12.012.
42. Mobile, M.; Widdowson, M.; Stewart, L.; Nyman, J.; Deeb, R.; Kavanaugh, M.; Mercer, J.; Gallagher, D. In-Situ Determination of Field-Scale NAPL Mass Transfer Coefficients: Performance, Simulation and Analysis. *J. Contam. Hydrol.* **2016**, *187*, 31–46, doi:10.1016/j.jconhyd.2016.01.010.
43. Yang, M.; Annable, M.D.; Jawitz, J.W. Field-Scale Forward and Back Diffusion through Low-Permeability Zones. *J. Contam. Hydrol.* **2017**, *202*, 47–58, doi:10.1016/j.jconhyd.2017.05.001.
44. Yang, M.; Annable, M.D.; Jawitz, J.W. Solute Source Depletion Control of Forward and Back Diffusion through Low-Permeability Zones. *J. Contam. Hydrol.* **2016**, *193*, 54–62, doi:10.1016/j.jconhyd.2016.09.004.
45. Yang, L.; Wang, X.; Mendoza-Sanchez, I.; Abriola, L.M. Modeling the Influence of Coupled Mass Transfer Processes on Mass Flux Downgradient of Heterogeneous DNAPL Source Zones. *J. Contam. Hydrol.* **2018**, *211*, 1–14, doi:10.1016/j.jconhyd.2018.02.003.
46. Anderson, M.R.; Johnson, R.L.; Pankow, J.F. Dissolution of Dense Chlorinated Solvents into Groundwater. 3. Modeling Contaminant Plumes from Fingers and Pools of Solvent. *Environ. Sci. Technol.* **1992**, *26*, 901–908, doi:10.1021/es00029a005.
47. Lee, K.Y.; Chrysikopoulos, C. V. NAPL Pool Dissolution in Stratified and Anisotropic Porous Formations. *J. Environ. Eng.* **1998**, *124*, 851–862, doi:10.1061/(ASCE)0733-9372(1998)124:9(851).
48. Atteia, O.; Höhener, P. Fast Semi-Analytical Approach to Approximate Plumes of Dissolved Redox-Reactive Pollutants in Heterogeneous Aquifers. 1. BTEX. *Adv. Water Resour.* **2012**, *46*, 63–73, doi:10.1016/j.advwatres.2011.10.003.
49. Atteia, O.; Höhener, P. Fast Semi-Analytical Approach to Approximate Plumes of Dissolved Redox-Reactive Pollutants in Heterogeneous Aquifers. 2: Chlorinated Ethenes. *Adv. Water Resour.* **2012**, *46*, 74–83, doi:10.1016/j.advwatres.2012.02.006.
50. Brown, G.H.; Brooks, M.C.; Wood, A.L.; Annable, M.D.; Huang, J. Aquitard Contaminant Storage and Flux Resulting from Dense Nonaqueous Phase Liquid Source Zone Dissolution and Remediation. *Water Resour. Res.* **2012**, *48*, 1–17, doi:10.1029/2011WR011141.
51. Henri, C. V.; Fernández-García, D. Toward Efficiency in Heterogeneous Multispecies Reactive Transport Modeling: A Particle-Tracking Solution for First-Order Network Reactions. *Water Resour. Res.* **2014**, *50*, 7206–7230, doi:10.1002/2013WR014956.
52. Adamson, D.T.; Chapman, S.W.; Farhat, S.K.; Parker, B.L.; DeBlanc, P.C.; Newell, C.J. Simple Modeling Tool for Reconstructing Source History Using High Resolution Contaminant Profiles From Low-k Zones. *Remediat. J.* **2015**, *25*, 31–51, doi:10.1002/rem.21431.

53. O'Carroll, D.; Sleep, B.; Krol, M.; Boparai, H.; Kocur, C. Nanoscale Zero Valent Iron and Bimetallic Particles for Contaminated Site Remediation. *Adv. Water Resour.* **2013**, *51*, 104–122, doi:10.1016/j.advwatres.2012.02.005.
54. Moody, C.A.; Field, J.A. Perfluorinated Surfactants and the Environmental Implications of Their Use in Fire-Fighting Foams. *Environ. Sci. Technol.* **2000**, *34*, 3864–3870, doi:10.1021/es991359u.
55. Saleh, N.; Sirk, K.; Liu, Y.; Phenrat, T.; Dufour, B.; Matyjaszewski, K.; Tilton, R.D.; Lowry, G. V. Surface Modifications Enhance Nanoiron Transport and NAPL Targeting in Saturated Porous Media. *Environ. Eng. Sci.* **2007**, *24*, 45–57, doi:10.1089/ees.2007.24.45.
56. He, F.; Zhao, D.; Paul, C. Field Assessment of Carboxymethyl Cellulose Stabilized Iron Nanoparticles for in Situ Destruction of Chlorinated Solvents in Source Zones. *Water Res.* **2010**, *44*, 2360–2370, doi:10.1016/j.watres.2009.12.041.
57. Yan, W.; Lien, H.-L.; Koel, B.E.; Zhang, W. Iron Nanoparticles for Environmental Clean-up: Recent Developments and Future Outlook. *Environ. Sci. Process. Impacts* **2013**, *15*, 63–77, doi:10.1039/C2EM30691C.
58. He, F.; Zhang, M.; Qian, T.; Zhao, D. Transport of Carboxymethyl Cellulose Stabilized Iron Nanoparticles in Porous Media: Column Experiments and Modeling. *J. Colloid Interface Sci.* **2009**, *334*, 96–102, doi:10.1016/j.jcis.2009.02.058.
59. Kim, H.; Hong, H.-J.; Jung, J.; Kim, S.-H.; Yang, J.-W. Degradation of Trichloroethylene (TCE) by Nanoscale Zero-Valent Iron (NZVI) Immobilized in Alginate Bead. *J. Hazard. Mater.* **2010**, *176*, 1038–1043, doi:10.1016/j.jhazmat.2009.11.145.
60. Sung, Y.; Ritalahti, K.M.; Sanford, R.A.; Urbance, J.W.; Flynn, S.J.; Tiedje, J.M.; Löffler, F.E. Characterization of Two Tetrachloroethene-Reducing, Acetate-Oxidizing Anaerobic Bacteria and Their Description as *Desulfuromonas Michiganensis* Sp. Nov. *Appl. Environ. Microbiol.* **2003**, *69*, 2964–2974, doi:10.1128/AEM.69.5.2964-2974.2003.
61. Liang, C.; Lee, I.-L.; Hsu, I.-Y.; Liang, C.-P.; Lin, Y.-L. Persulfate Oxidation of Trichloroethylene with and without Iron Activation in Porous Media. *Chemosphere* **2008**, *70*, 426–435, doi:10.1016/j.chemosphere.2007.06.077.
62. Aulenta, F.; Catervi, A.; Majone, M.; Panero, S.; Reale, P.; Rossetti, S. Electron Transfer from a Solid-State Electrode Assisted by Methyl Viologen Sustains Efficient Microbial Reductive Dechlorination of TCE. *Environ. Sci. Technol.* **2007**, *41*, 2554–2559, doi:10.1021/es0624321.
63. Zheng, C.; Wang, P.P. *MT3DMS: A Modular Three-Dimensional Multispecies Transport Model for Simulation of Advection, Dispersion, and Chemical Reactions of Contaminants in Groundwater Systems; Documentation and User's Guide*; Alabama Univ University, 1999;
64. Batu, V. *Applied Flow and Solute Transport Modeling in Aquifers: Fundamental Principles and Analytical and Numerical Methods*; CRC Press, 2005; ISBN 1420037471.
65. Zheng, C.; Bennett, G.D. *Applied Contaminant Transport Modeling*; 2nd ed.; Wiley-Interscience: New York, 2002; ISBN 978-0-471-38477-9.
66. Powers, S.E.; Abriola, L.M.; Weber, W.J. An Experimental Investigation of Nonaqueous Phase Liquid Dissolution in Saturated Subsurface Systems: Transient Mass Transfer Rates. *Water Resour. Res.* **1994**, *30*, 321–332, doi:10.1029/93WR02923.
67. Zhu, J.; Sykes, J. The Influence of NAPL Dissolution Characteristics on Field-Scale Contaminant Transport in Subsurface. *J. Contam. Hydrol.* **2000**, *41*, 133–154, doi:10.1016/S0169-7722(99)00064-9.
68. Clement, T.P.; Johnson, C.D.; Sun, Y.; Klecka, G.M.; Bartlett, C. Natural Attenuation of Chlorinated Ethene Compounds: Model Development and Field-Scale Application at the Dover Site. *J. Contam. Hydrol.* **2000**, *42*, 113–140, doi:10.1016/S0169-7722(99)00098-4.

69. Clement, T.P. *RT3D, A Modular Computer Code for Simulating Reactive Multi- Species Transport in 3-Dimensional Groundwater Systems*; Washington, 1997;
70. Burnell, D.K.; Hansen, S.K.; Xu, J. Transient Modeling of Non-Fickian Transport and First-Order Reaction Using Continuous Time Random Walk. *Adv. Water Resour.* **2017**, *107*, 370–392, doi:10.1016/j.advwatres.2017.06.014.
71. Burnell, D.K.; Xu, J.; Hansen, S.K.; Sims, L.S.; Faust, C.R. A Practical Modeling Framework for Non-Fickian Transport and Multi-Species Sequential First-Order Reaction. *Groundwater* **2018**, *56*, 524–540, doi:10.1111/gwat.12660.
72. Comolli, A.; Hidalgo, J.J.; Moussey, C.; Dentz, M. Non-Fickian Transport Under Heterogeneous Advection and Mobile-Immobile Mass Transfer. *Transp. Porous Media* **2016**, *115*, 265–289, doi:10.1007/s11242-016-0727-6.
73. Aria, M.; Cuccurullo, C. Bibliometrix : An R-Tool for Comprehensive Science Mapping Analysis. *J. Informetr.* **2017**, *11*, 959–975, doi:10.1016/j.joi.2017.08.007.
74. Riehmman, P.; Hanfler, M.; Froehlich, B. Interactive Sankey Diagrams. In Proceedings of the IEEE Symposium on Information Visualization, 2005. INFOVIS 2005.; IEEE, 2005; pp. 233–240.
75. Aria, M.; Misuraca, M.; Spano, M. Mapping the Evolution of Social Research and Data Science on 30 Years of Social Indicators Research. *Soc. Indic. Res.* **2020**, *149*, 803–831, doi:10.1007/s11205-020-02281-3.
76. Xiao, Z.; Qin, Y.; Xu, Z.; Antucheviciene, J.; Zavadskas, E.K. The Journal Buildings: A Bibliometric Analysis (2011–2021). *Buildings* **2022**, *12*, 37, doi:10.3390/buildings12010037.